



Heterogeneous & Homogeneous & Bio- & Nano-

CHEM **CAT** CHEM

CATALYSIS

Accepted Article

Title: Highly efficient photo-reduction of p-nitrophenol by protonated graphitic carbon nitride nanosheets

Authors: Jiajia Qian, Aili Yuan, Chengkai Yao, Jiyang Liu, Benxia Li, Fengna Xi, and Xiaoping Dong

This manuscript has been accepted after peer review and appears as an Accepted Article online prior to editing, proofing, and formal publication of the final Version of Record (VoR). This work is currently citable by using the Digital Object Identifier (DOI) given below. The VoR will be published online in Early View as soon as possible and may be different to this Accepted Article as a result of editing. Readers should obtain the VoR from the journal website shown below when it is published to ensure accuracy of information. The authors are responsible for the content of this Accepted Article.

To be cited as: *ChemCatChem* 10.1002/cctc.201801146

Link to VoR: <http://dx.doi.org/10.1002/cctc.201801146>

WILEY-VCH

www.chemcatchem.org



Highly efficient photo-reduction of *p*-nitrophenol by protonated graphitic carbon nitride nanosheets

Jiajia Qian, Aili Yuan, Chengkai Yao, Jiyang Liu, Benxia Li, Fengna Xi, and Xiaoping Dong*

Abstract: Photocatalytic reduction of *p*-nitrophenol to *p*-aminophenol is of significant importance because of the high toxicity of *p*-nitrophenol and the wide application of *p*-aminophenol. Graphitic carbon nitride (g-CN) is an excellent photocatalyst for various photo-reduction reactions, but inefficient for photo-reduction of *p*-nitrophenol due to the electrostatic exclusion. In this work, we control the morphology and surface property of g-CN and achieve significantly enhanced activity. The obtained protonated g-CN nanosheet (pg-CNNS) material has positively charged surface that can adsorb *p*-nitrophenolate anions, therefore facilitating the transfer of photo-generated electrons from catalyst to *p*-nitrophenol. Its reaction rate is 1626 times higher than that of the pristine g-CN. Besides the surface charge, the morphology of photocatalyst also has important effect on activity, which is demonstrated by the relatively low activity of protonated g-CN in comparison to pg-CNNS. The pg-CNNS photocatalyst has an excellent stability and superior catalytic universality for photo-reduction of various nitroaromatic compounds. This work does not only expand the application of a well-known material, but also highlights the importance of understanding photocatalytic mechanism for designing photocatalyst.

Introduction

Because of the high toxicity, nocuity, poor biodegradability and wide application in industries, nitroaromatic compounds have been considered as priority within harmful environmental pollutants.^[1,2] Among numerous nitroaromatic compounds, *p*-nitrophenol (PNP) is one of the most frequently occurring by-products in various industries, and its removal from environment is very important.^[3-5] In comparison to the energy-consuming and inefficient strategies, the catalytic reduction of PNP to low toxic *p*-aminophenol (PAP) under mild condition has attracted enormous attentions.^[6-10] More importantly, the reduced product (PAP) is a vital intermediate for synthesis of many medicines^[10-13] and precursor for various chemicals.^[14-17]

The most popular route for reducing nitroaromatic compounds to corresponding aniline derivatives is catalytic hydrogenation by heterogeneous catalysts.^[18] However, this process is usually performed at relatively high temperature and is hard to selectively reduce nitro groups if additional reducible functionalities are modified on aromatics. Recently, catalytic reduction of nitroaromatic compounds in mild condition has achieved significant progress by noble metal catalysts (Au, Ag, Pt, Pd and so on) using NaBH₄ as reductant.^[19-23] Especially, the reaction of PNP to PAP has become a model to evaluate the activity of catalysts.^[24]

As a green and energy-saving technique, semiconductor photocatalysis using solar irradiation has been extensively employed to transformation of organic compounds during the oxidation or reduction process.^[25,26] The photo-excited electrons on conduction band (CB) of photocatalysts with strong reducible property can also reduce PNP to PAP. Nevertheless, the correspondingly photo-generated holes on valence band (VB) are highly oxidizing, which will photo-oxidize organic molecules including PNP. Additionally, besides the insufficient utilization of solar light the conventional semiconductor photocatalyst of TiO₂ has a low CB potential that results in the photo-induced electrons cannot efficiently reduce PNP.^[27] Modification with noble metals on TiO₂ has been demonstrated which is profitable for the enhancement of photo-reduction activity.^[11] However, the high cost of noble metal limits the practical application of these photocatalysts. On the other hand, to improve the photocatalytic behavior of PNP reduction, the competitive oxidation reaction of PNP by photo-generated holes must be suppressed. In general, reactants, such as NaBH₄, Na₂SO₃ and hydrazine, are used as scavengers to quench holes.^[28-30]

Graphitic carbon nitride (g-CN) is a fascinating polymeric organic semiconductor photocatalyst of tri-s-triazine with distinct advantages, for instance the low-cost precursors, facile synthetic process, high chemical stability and metal-free nature.^[31-39] Furthermore, g-CN has good visible-light response and a narrow band gap of 2.6~2.8 eV. The CB position of g-CN is much higher than those of conventional photocatalysts, meaning it has much stronger reduction ability. Consequently, g-CN presents excellent photocatalytic performance for photo-reduction reactions, such as hydrogen evolution from water splitting and reduction of CO₂ to solar fuels.^[31-35] However, it is noteworthy that the photocatalytic activity of g-CN for reduction of PNP to PAP is extremely low.^[40,41] Moreover, in comparison to the numerous investigation interests on other photocatalytic reactions by g-CN or g-CN based composites, fewer studies have been reported on photo-reduction of PNP. And, in most cases g-CN was only used as photo-reduction medium or supporter to prepare or load noble metal catalysts.^[40-42]

To obtain high photo-reduction efficiency, the photo-excited electron-hole pairs should be sufficiently separated and then the photo-generated electrons must be rapidly transported from g-CN to PNP. With the co-presence of PNP and conventional reductants or hole scavengers (NaBH₄, hydrazine or Na₂SO₃), PNP would be transformed to *p*-nitrophenolate anion. However, under such condition the surface of g-CN is negatively charged. As consequence, *p*-nitrophenolate anion cannot be adsorbed onto the catalyst surface, therefore limiting the transferring efficiency of photo-induced electrons to PNP. Herein, we report a significant enhancement of photocatalytic PNP reduction by pure g-CN during controlling its morphology and surface property. Positively charged g-CN nanosheet material is synthesized by H₂SO₄ exfoliation and meanwhile protonation process. The obtained protonated g-CN nanosheet (pg-CNNS) catalyst has a high activity for photo-reduction of PNP under

J. Qian, A. Yuan, C. Yao, Prof. J. Liu, Prof. B. Li, Prof. F. Xi, Prof. X. Dong
Department of Chemistry
Zhejiang Sci-Tech University
928 Second Avenue, Xiasha Higher Education Zone, Hangzhou, China
E-mail: xpdong@zstu.edu.cn

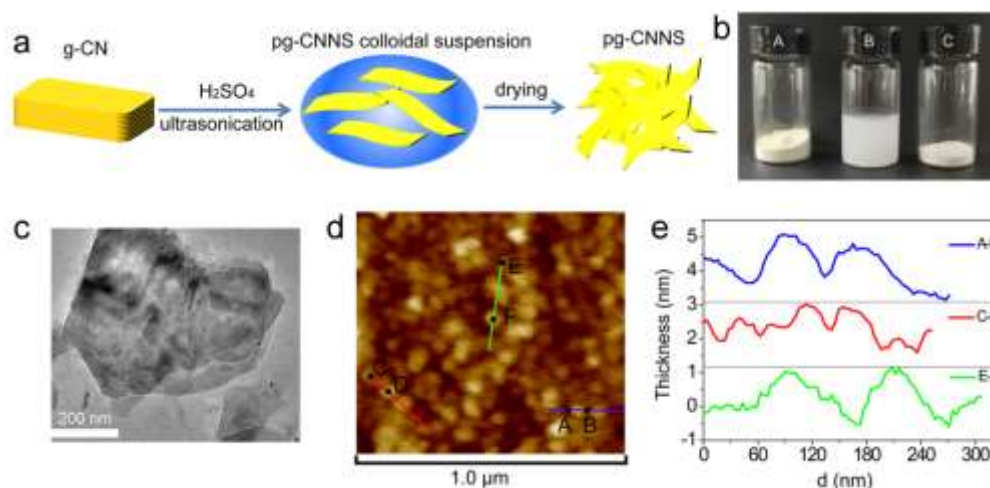


Figure 1. (a) Schematic illustration for the delamination of g-CN into pg-CNNS by concentrated H_2SO_4 ; (b) Photographs of (A) g-CN, (B) pg-CNNS suspension and (C) collected pg-CNNS; (c) TEM and (d) AFM images of pg-CNNS. (e) The height profile of colored lines in (d).

visible light irradiation and its reaction rate is 1626 times higher than that of the pristine g-CN. Furthermore, it has high stability and reusability, as well as excellent universality that various substituted nitroaromatic compounds can be efficiently photo-reduced to their corresponding aminoaromatic compounds.

Results and Discussion

1. Physicochemical properties of pg-CNNS photocatalyst

The 2D pg-CNNS photocatalyst is prepared by delamination of the pristine g-CN in sulphuric acid under ultrasonic treatment (Figure 1a). In comparison to the bulky powder of g-CN (Figure 1b), the exfoliated pg-CNNS is stable in a colloidal suspension. These nanosheets can be collected by evaporating water, and the solid sample presents a much more delicate color than g-CN, which may be related to the protonation effect of carbon

nitride.^[43-46] A nanosheet-like aspect of pg-CNNS is illustrated in the transmission electron microscopy (TEM) image (Figure 1c). The size and thickness of the pg-CNNS were examined by atomic force microscope (AFM, Figure 1d) and its corresponding height profiles (Figure 1e). It can be seen that uniform nanosheets have been formed through the exfoliation processes, which give an average thickness of 1.0 ± 0.2 nm, corresponding to 3–4 layers of 2D CN skeleton. The change of surface group was measured by Fourier transform infrared (FTIR) technology, as revealed in Figure S1. Absorptions at the range of 1200–1600 cm^{-1} and 810 cm^{-1} are characteristic peaks of graphitic carbon nitride.^[36, 37] There is no apparent spectral difference between g-CN and pg-CN, suggesting the protonation does not influence the skeleton of CN heterocycle. However, some of these absorptions of 1200–1600 cm^{-1} change after the H_2SO_4 treatment. It should result from the partial oxidation of CN framework by H_2SO_4 and the absorption band at ~ 1600 cm^{-1} shifting to the low

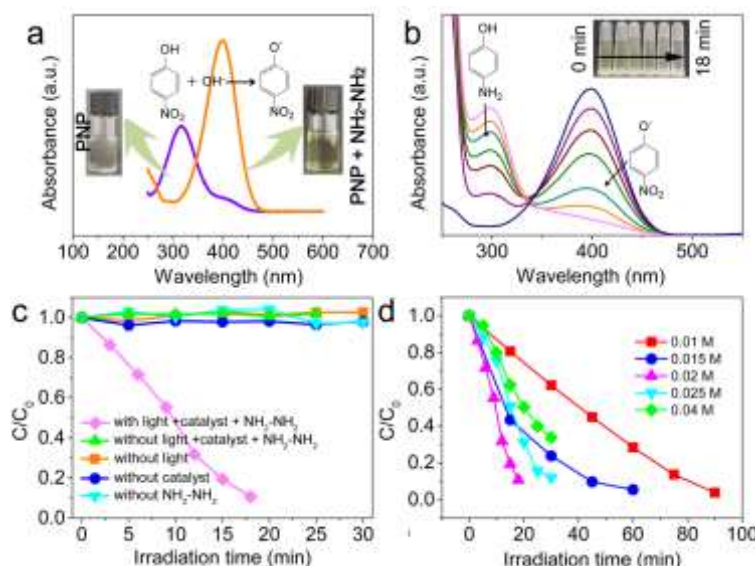


Figure 2. (a) UV-vis spectra of PNP before and after addition of hydrazine; (b) The spectral change of PNP solution with hydrazine by the photocatalytic treatment of pg-CNNS ($\lambda > 420$ nm); (c) Photocatalytic performance under various reaction condition; (d) Photocatalytic performance of pg-CNNS for reduction of PNP with various hydrazine concentrations.

wavenumber region in pg-CNNS is ascribed to the presence of carboxylate groups.^[44] Figure S2 compares X-ray diffraction (XRD) patterns of g-CN, pg-CN and pg-CNNS samples. Two pronounced diffractions at 13.1° and 27.6° in patterns respectively correspond to the in-planar (100) diffraction and the interlayer (002) diffraction of the graphite-like structure of carbon nitride.^[36,37] The pg-CNNS shows a weak broad interlayer (002) peak, which is attributed to its few-layer structure. Moreover, the (002) diffraction of pg-CNNS slightly shifts to higher angle compared to g-CN and pg-CN, reflecting the decreased interlayer spacing and a structural compaction that is similar to the reported reference.^[45] N₂ adsorption-desorption isotherms of g-CN, pg-CN and pg-CNNS are shown in Figure S3. The pg-CNNS has a much more marked leap at the high P/P₀ range (0.8–1.0) than g-CN and pg-CN, demonstrating its much more developed porosity. In general, ultrathin 2D nanosheets have large surface area. However, once drying them into solids, these 2D nanosheets would re-stack and result in diminishing specific surface area. Even so, the re-stacked pg-CNNS still presents much higher specific surface area (25.7 m² g⁻¹) than g-CN and pg-CN (8.1 m² g⁻¹ and 8.8 m² g⁻¹).

2. Enhanced photocatalytic performance of pg-CNNS for PNP reduction

The activities of photocatalysts for PNP photo-reduction were carried out under visible light irradiation (>420 nm). As described in Figure 2a, aqueous solution of PNP shows an absorption peak centered at 317 nm. After adding hydrazine into the PNP solution, the absorption peak shifts to 400 nm, which is ascribed to the transformation of PNP to *p*-nitrophenolate ions by the reaction of acidic phenol hydroxyl group and alkaline hydrazine. Meanwhile, the color of the solution changes from light yellow to dark yellow. With the presence of the pg-CNNS sample, the characteristic peak of the aqueous *p*-nitrophenolate ion rapidly declines under visible light illumination, and correspondingly the solution becomes colorless (Figure 2b). At the meantime, a new absorption with peak centered at 298 nm that is related to PAP appears and gradually strengthens with the increase of irradiation time. The conversion ratio of PNP under various conditions is presented in Figure 2c. PNP is very stable and almost no PNP conversion happens without catalyst and hydrazine in dark. As the single factor (catalyst, hydrazine and illumination) absences in the reaction, the PNP conversion ratio

Table 1. Composition analysis of solution after photocatalytic reaction under different reaction condition by HPLC

Reaction condition	PNP (retention time of 8.80 min)	PAP (retention time of 2.41 min)
1		✓
2	✓	
3	✓	
4	✓	
5	✓	

Essentia LC-15C; detector: SPD-15C; column: WondaSil C18, 4.6 × 200 mm, 5μm; flow: 0.9 mL min⁻¹, V (CH₃CN/H₂O) = 3/7

1: With light + Catalyst + NH₂-NH₂; 2: Without light + Catalyst + NH₂-NH₂
3: Without light; 4: Without catalyst; 5: Without NH₂-NH₂

is also extremely low (< 5%). These results imply that light irradiation, hydrazine and photocatalyst are necessities for the efficient reduction of PNP. The reaction process was also monitored by high-performance liquid chromatography (HPLC, Figure S4 and Table 1). The peak at 2.15 min only appears in the reaction systems with pg-CNNS that is from the adsorbed sulfate ions. The other two peaks are respectively assigned to PNP (retention time of 8.80 min) and PAP (retention time of 2.41 min) in these HPLC spectra, which demonstrates that no by-products were produced. It is found that the signal at the retention time of 2.41 min does not appear without the condition of visible light irradiation, photocatalyst or hydrazine, indicating that these three factors are vital for the photocatalytic reduction of PNP. With the presence of photocatalyst and hydrazine under visible light irradiation, all of PNP are reduced to PAP, which is revealed by the disappearance of PNP peak.

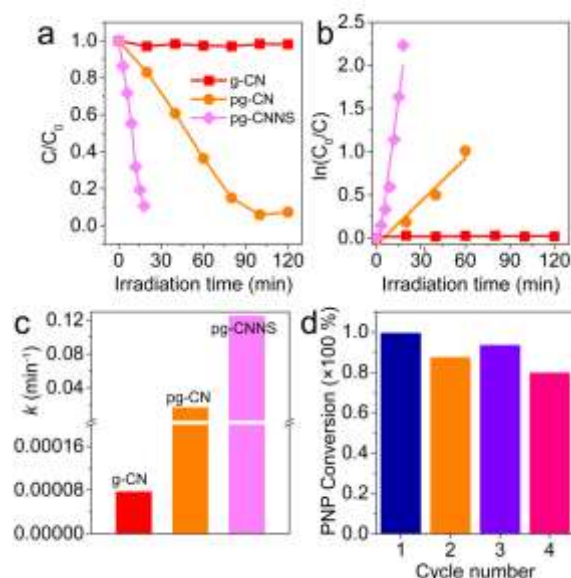


Figure 3. (a) Comparison for the photocatalytic activity of pg-CNNS with g-CN and pg-CN, and (b) their corresponding pseudo-first-order kinetics data and (c) apparent rate constants; (d) The durability property of pg-CNNS for photo-reduction of PNP.

Table 2. Comparison for photocatalytic performance of pg-CNNS with reported photocatalysts

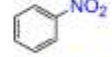
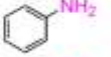
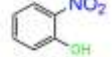
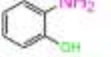
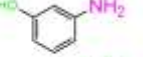
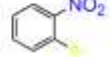
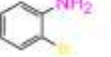
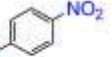
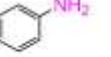
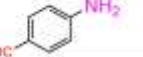
Catalysts	Reducer	Reaction time (min)	Conversion (%)	TOF (10^{-2} h^{-1})	Reference
pg-CNNS	hydrazine	18	100	2	This work
g-C ₃ N ₄ -N	NaBH ₄	60	0	-	[41]
C ₃ N ₄ -ZnS	Na ₂ SO ₃	240	100	0.28	[47]
CdS/g-C ₃ N ₄	alcohol	160	25	0.98	[48]
Cu ₂ O-rGO-C ₃ N ₄	Na ₂ SO ₃	60	80	-	[49]
CdS	Na ₂ SO ₃	180	100	0.93	[50]
TiO ₂	NaBH ₄	180	0	-	[51]
RGO-ZnS	NaBH ₄	70	80	0.143	[52]
Fluorinated TiO ₂	Na ₂ SO ₃	270	90	0.80	[30]
Ce ₂ Zr ₂ O ₇ @rGO	NaBH ₄	120	100	1	[53]
ZrO ₂ -TiO ₂	Na ₂ SO ₃	300	100	0.27	[54]

Hydrazine is usually used as nucleophilic reagent due to the existence of lone pairs in nitrogen atoms. This would result in a possibly competing adsorption of hydrazine with *p*-nitrophenolate anion on the positively charged surface of pg-CNNS. Thus, the concentration of hydrazine is of great importance for this photocatalytic reaction. As shown in Figure 2d, the photocatalytic activity of pg-CNNS is significantly improved as increasing the hydrazine concentration from 0.01 M to 0.02 M, and gradually weakens as the concentration of hydrazine is increased from 0.02 M to 0.04 M. At a low hydrazine concentration, the adsorbed hydrazine would be rapidly oxidized by photo-induced holes to molecular nitrogen and protons. However, at a high concentration, the adsorbed hydrazine cannot be immediately oxidized. It would prohibit the adsorption of PNP onto the surface of pg-CNNS, thus decreasing the photocatalytic efficiency. We consequently employed 0.02 M hydrazine as the optimized reaction condition.

The photocatalytic reduction activity of pg-CNNSs is compared with other graphitic carbon nitride materials, including g-CN and pg-CN. As exhibited in Figure 3a, g-CN displays very poor photocatalytic performance and no obvious photo-reduction happens within 120 min irradiation. By tuning the surface charge of carbon nitride to positive, the pg-CN sample shows an apparently improved activity, where ~95 % PNP is transformed to PAP after 120 min illumination. We attribute this improvement to the facilitating adsorption of *p*-nitrophenolate anions on the positively charged surface of pg-CN. With the increase of positively charged surface area, the photo-reduction performance is further enhanced by the pg-CNNS photocatalyst, and a complete conversion of PNP is realized after 18 min reaction. A well linear fitting of photocatalytic data ($\ln C_0/C$ vs. t) is depicted in Figure 3b, suggesting this photocatalytic reduction process follows the first-order kinetics. The apparent rate

constant (k) of pg-CNNS is 0.125 min^{-1} , which is about 1626, 7.5 times higher than those of g-CN and pg-CN, respectively (Figure 3c). Additionally, various concentrations of PNP were attempted in this work, and the result reveals that the pg-CNNS photocatalyst even can efficiently reduce PNP in high concentration (20 mg L^{-1}) to PAP (Figure S5). We also compare the photocatalytic performance of pg-CNNS with these reported photocatalysts in references (Table 2). The calculated value of turn over frequency (TOF) is 0.02 h^{-1} for pg-CNNS that is much higher than those estimated from reference results. To evaluate the stability and reusability of pg-CNNS, the successive run was performed by directly adding a certain amount of PNP in the post-reacted solution without further treatment of photocatalyst. Figure 3d illustrates the PNP conversion efficiency of four cycles, where ~80 % conversion of PNP is retained at the 4th run

Table 3. Photocatalytic activity of pg-CNNS for different group substituted nitroaromatic compounds.

Entry	Substrate	Product	Conversion (%)
1			100
2			100
3			100
4			100
5			100
6			100

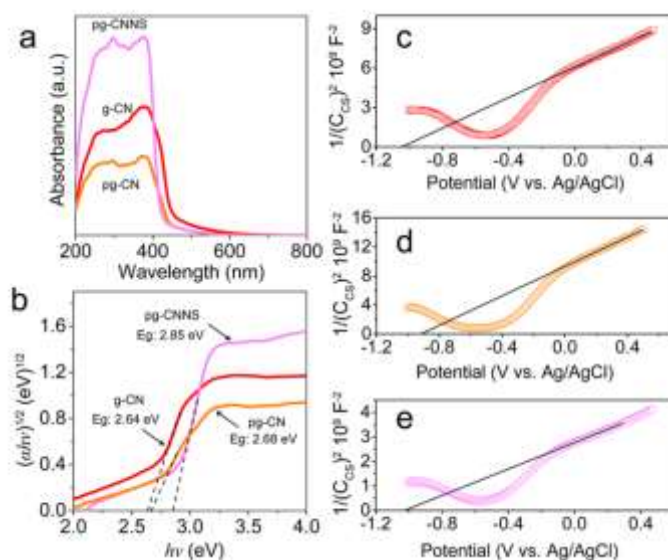


Figure 4. (a) UV-vis DRS of g-CN, pg-CN and pg-CNNS; (b) The plots of $(\alpha hv)^{1/2}$ vs $h\nu$. Mott-Schottky curves of (c) g-CN, (d) pg-CN and (e) pg-CNNS.

implying its superior reusability. Other nitroaromatic chemicals were also employed to estimate the photocatalytic universality of pg-CNNS. As listed in Table 3, different group substituted nitroaromatic compounds, *o*-nitrophenol, *m*-nitrophenol, nitrobenzene, *p*-nitrobenzoic acids, *p*-nitrochlorobenzene and *o*-bromonitrobenzene, also present sufficient conversion to corresponding reductive aminoaromatic products by the photocatalytic reaction of pg-CNNS under visible light irradiation.

3. Possible photocatalytic mechanism of pg-CNNS for reduction of PNP

For well understanding the enhanced photocatalytic

performance of pg-CNNS, we firstly tried to plot the band alignment of photocatalysts. The optical properties of the as-prepared g-CN, pg-CN and pg-CNNS samples were examined using UV-vis diffuse reflectance spectroscopy (DRS) technology. As shown in Figure 4a, the pristine g-CN exhibits an absorption edge of ~450 nm that represents a band gap (E_g) of 2.64 eV (Figure 4b). The subsequent protonation treatment makes the absorption edge slightly shift to the short wavelength region that is in accordance with the results in published literatures.^[44] And accordingly, the E_g of pg-CN is estimated to 2.68 eV. Due to the quantum confinement effect of few-layer structure and the protonation as well, the absorption spectrum of pg-CNNS

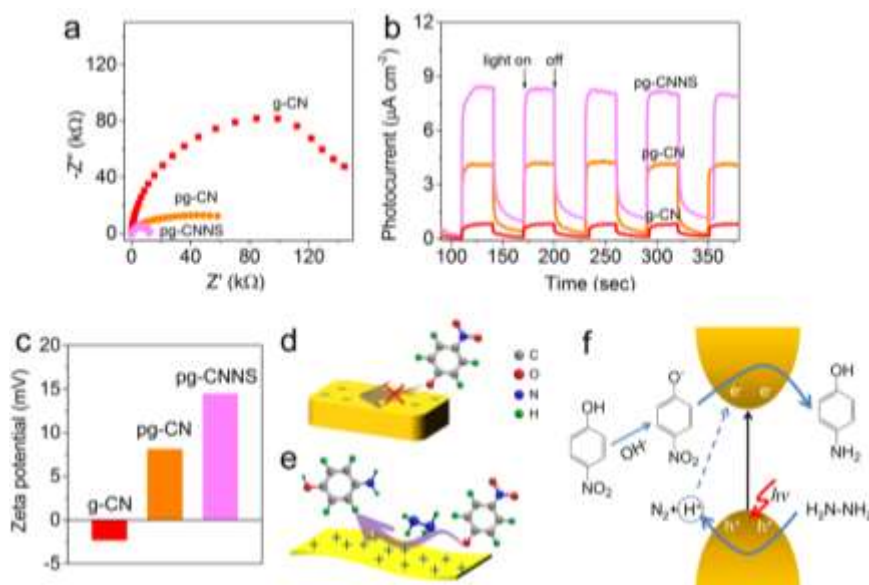


Figure 5. (a) EIS curves, (b) transient photocurrent responses and (c) zeta potentials of g-CN, pg-CN and pg-CNNS; Schematic illustration for (d) electrostatic exclusion of *p*-nitrophenolate anions by the negatively charged g-CN surface, (e) adsorption of *p*-nitrophenolate anions on the positively charged pg-CNNS surface and (f) the possible photocatalytic mechanism of pg-CNNS for photocatalytic reduction of PNP to PAP.

illustrates a much more obvious blue-shift, and the E_g is enlarged to 2.85 eV.

The electrochemical Mott-Schottky (MS) technique is an effective route to determine the conduction behavior of semiconductor and its flat-band potential (E_{fb}) that can be regarded as the Fermi level (E_F). Similar MS curves of g-CN, pg-CN and pg-CNNS (Figure 4c-e) suggest their similar electronic structure and conduction behavior. Also, the n type semiconductor behavior is consistent with these previous results.^[55] The E_{fb} values of g-CN, pg-CN and pg-CNNS are the X-axis intercepts of prolonging tangents that are evaluated to be -1.02 eV, -0.90 eV and -1.01 eV vs. Ag/AgCl, respectively. Thus, associated with their E_g values the band alignment of photocatalysts is plotted in Figure S6. Compared to the pristine g-CN, the protonated sample has a low conduction band (CB) edge potential. This result demonstrates the low activity of g-CN does not result from the low reduction ability of photo-generated electrons.

Electrochemical impedance spectroscopy (EIS) was performed to study the transfer and separation of photo-excited carriers. As revealed in Figure 5a, the Nyquist plot of pg-CNNS shows a much smaller semi-cycle than those of pg-CN and g-CN, which reflects a smaller R_{ct} (charge transfer resistance).^[56] Figure 5b exhibits the photocurrent responses of photocatalysts during repeated on-off cycles under visible-light irradiation. It is obviously found that the pg-CNNS sample has the most strongest photocurrent density, because the ultrathin structure of pg-CNNS provides short diffusion distance for photo-excited charges to rapidly transport to surface. Moreover, the small R_{ct} of pg-CNNS represents a fast interfacial charge transfer, which may be responsible for the superior performance for PNP reduction. Besides, surface potential of materials were measured, and the results are shown in Figure 5c. A zeta potential of -2.30 mV suggests that g-CN possesses negative polarity on its surface. With the protonation treatment the surface charge of pg-CN is changed from negative to positive (+8.10 mV). As undergoing exfoliation and meanwhile protonation, the pg-CNNS sample supports much more positive charges (+14.47 mV) on surface than pg-CN.

In view of above results, we propose a possible mechanism of pg-CNNS for photo-reduction of PNP with hydrazine. As an alkaline compound, hydrazine will react with PNP to produce *p*-nitrophenolate anion that cannot be adsorbed onto the negatively charged surface of g-CN (Figure 5d), therefore suppressing the transfer of photo-induced electron to substrate molecules. Because the exfoliation of pristine g-CN is carried out in a sulphuric acid system, the terminal amino groups on the obtained pg-CNNS would accept protons to form positive ammonium ions. Consequently, *p*-nitrophenolate anions facilitate access to the surface of pg-CNNS and are reduced to PAP with hydrazine (Figure 5e). The detailed photocatalytic process is illustrated in Figure 5f. Under visible light illumination, electrons on the VB of pg-CNNS are excited and transmitted to its CB, meanwhile leaving holes on the VB. These photo-generated charges can fastly diffuse to the surface due to the extremely thin morphology of pg-CNNS, which is favorable for diminishing the bulk recombination of electron-hole pairs. Then, these surface

holes with strong oxidative ability are captured by hydrazine to produce N_2 and H^+ . On the other hand, the photo-induced electrons transfer to the nitro group of PNP that is tightly adsorbed on the pg-CNNS surface, and subsequently, amination reaction takes place by absorbing H^+ ions from the oxidation of hydrazine.

Conclusions

In summary, we have realized the efficient conversion of PNP to PAP by an inactive photocatalyst of graphitic carbon nitride for this reaction. The pristine g-CN shows poor photocatalytic ability for PNP reduction because its bulky morphology results in the high charge recombination rate and the negatively charged surface will exclude *p*-nitrophenolate anions. After exfoliating it into 2D nanosheets by sulphuric acid, the 2D pg-CNNS sample presents an ultrathin morphology and its surface loads plentiful positive charges, where the photo-excited charges are sufficiently separated, fast transport to the surface, as well as subsequently transfer onto the adsorbed *p*-nitrophenolate anions to form reduced PAP. Its photo-reduction rate is 1626, 7.5 times higher than those of g-CN and pg-CN, respectively. Moreover, the pg-CNNS has well photocatalytic reusability and also has superb activity for reduction of other functionalized nitroaromatic chemicals. This work indicates the surface property of photocatalysts is of vital importance to photocatalytic reaction, especially to the reduction process because photo-excited electrons are only able to transfer to the adsorbed molecules. Additionally, this work will inspire us to attempt other photo-reduction reactions for negative substrates using this protonated carbon nitride nanosheet photocatalyst, such as transforming Cr (VI) to Cr (III).

Experimental Section

1 Synthesis of photocatalysts

The g-CN was obtained by thermal polycondensation of melamine, which was reported in our previous literatures.^[43] And protonated g-CN (pg-CN) was synthesised by treating 3 g g-CN with 60 mL HCl aqueous solutions (12 mol L^{-1}), similar with reported method.^[44] The pg-CNNS was prepared by the treatment of g-CN with H_2SO_4 . Typically, 2 g g-CN powder was added into 40 mL of H_2SO_4 (98 wt%) and stirred for 10 h at room temperature. Then, the mixture was slowly poured into 100 mL of deionized water and sonicated with 8h for exfoliation. After pouring off the clear supernatant, the sediments were rinsed by water again and again. As most of the deposition could not be separated from the suspension by centrifugation at 12000 rpm, we achieved the stable colloidal suspension of pg-CNNS. Finally, the pg-CNNS powder was obtained by drying at 70 °C overnight.

2 Characterizations

Transmission electron microscope (TEM) image was taken on a JEOL-2100 electron microscope operating at an accelerating voltage of 200 kV. The samples were characterized by X-ray powder diffraction (XRD) by a DX-2700 diffractometer (Dandong Haoyuan Instrument Co. Ltd. China). The thickness was assessed using a tapping mode atomic force microscope (AFM) (Multimode-8; Bruker; USA). Fourier transform infrared (FTIR) spectra were recorded on a Nicolet 5700 spectrophotometer using the standard KBr disk method. Nitrogen sorption measurements were carried out at $-196\text{ }^{\circ}\text{C}$ on a micromeritics ASAP 2020 analyzer, and the specific surface area (S_{BET}) was evaluated using the Brunauer-Emmett-Teller (BET) method. UV-vis absorption spectra and diffuse reflectance spectra (DRS) were recorded on a Shimadzu 2450 UV-vis spectrometer with an integrating sphere using BaSO₄ as the reference. The reaction process was monitored by high-performance liquid chromatography (HPLC; Shimadzu, LC-20AT). The electrochemical tests were performed on a CHI660E electrochemical workstation (Chenhua, Shanghai, China). The zeta potentials of different samples were measured with Malvern Nano ZS90.

3 Photocatalytic tests

The photo-reduction activities of photocatalysts were evaluated by the reduction of PNP in aqueous solution under visible light irradiation using a 300 W xenon lamp (HSX-F300, Beijing NBet) with a 420 nm cutoff filter as the light source. In each experiment, 100 mg of catalyst was added to an aqueous solution (100 mL) of PNP (5 mg L^{-1}) containing 0.02 M hydrazine in a beaker. Prior to irradiation, the catalyst was stirred in the dark for 60 min to ensure the establishment of adsorption-desorption equilibrium. And the air in reactor was removed by pure N₂. At given time intervals, 3.5 mL of the solution was collected and subsequently centrifuged to remove the particles. The concentration of solution was analyzed by measuring the maximum absorbance at 400 nm for *p*-nitrophenolate ions through a Shimadzu UV-2450 spectrophotometer. The TOF is calculated as the number of PAP mass (g) evolved per gram of total catalyst per unit of time (h): $\text{TOF} = m_{\text{PAP}}/(m_{\text{catalyst}} \cdot t)$.

4 Photo-electrochemical measurements

The photo-electrochemical properties were studied on an electrochemical station (CHI660E, Chenhua, Shanghai, China) linked with computer. The Ag/AgCl electrode, platinum foil and Na₂SO₄ (0.2 M) were employed as reference electrode, counter electrode and electrolyte solution, respectively. The working electrode was fabricated as follow: 20 mg catalyst was ultrasonically dispersed in 2 mL distilled water for 0.5 h, and then the obtained suspension was coated on a 3 cm × 1 cm indium tin oxide (ITO) glass before drying at 70 °C for 12 h.

Acknowledgements

This work was financially supported from the financial support from the Zhejiang Provincial Natural Science Foundation of China (No. LY17B010004, LY17B050007) and the 521 talent project of ZSTU.

Keywords: Nanosheets • P-Aminophenol • Photocatalytic Reduction • P-Nitrophenol • Protonated Graphitic Carbon Nitride

- [1] K. Ju, E. Rebecca, *Mol. Boil. R.* **2010**, *5*, 250-272.
 [2] J. Spain, *Annu. Rev. Microbiol.* **1995**, *49*, 523-555.

- [3] L. Yang, S. Luo, Y. Li, Y. Xiao, Q. Kang, Q. Cai, *Environ. Sci. Technol.* **2010**, *44*, 7641-7646.
 [4] J. Feng, L. Su, Y. Ma, C. Ren, Q. Guo, X. Chen, *Chem. Eng. J.* **2013**, *221*, 16-24.
 [5] M. Rocha, P. Costa, C. Sousa, C. Pereira, J. Rodríguez-Borges, C. Freire, *J. Catal.* **2018**, *361*, 143-155.
 [6] J. Lee, J. Park, H. Song, *Adv. Mater.* **2008**, *20*, 1523-1528.
 [7] J. Das, M. Aziz, H. Yang, *J. Am. Chem. Soc.* **2006**, *128*, 16022-16023.
 [8] C. Lin, K. Tao, D. Hua, Z. Ma, S. Zhou, *Molecules* **2013**, *18*, 12609-12620.
 [9] N. Pradhan, A. Pal, T. Pal, *Colloids Surf., A* **2002**, *196*, 247-257.
 [10] Chang, Y. Luo, W. Lu, X. Qin, A. Asiri, A. Al-Youbi, X. Sun, *Catal. Sci. Technol.* **2012**, *2*, 800-806.
 [11] M. Mohamed, M. Sharif, *Appl. Catal. B: Environ.* **2013**, *142*, 432-441.
 [12] G. Falcone, O. Giuffrè, S. Sammartano, *J. Mol. Liq.* **2011**, *159*, 146-151.
 [13] S. Bawane, S. Sawant, *Appl. Catal. A* **2015**, *293*, 162-170.
 [14] A. Saha, B. Ranu, *J. Org. Chem.* **2008**, *73*, 6867-6870.
 [15] A. Rahman, S. Jonnalagadda, *Catal. Lett.* **2008**, *123*, 264-268.
 [16] F. Cardenas-Lizana, S. Gomez-Quero, M. Keane, *Catal. Commun.* **2008**, *9*, 475-481.
 [17] A. Vass, J. Dudás, J. Tóth, R. Varma, *Tetrahedron Lett.* **2001**, *42*, 5347-5349.
 [18] S. Cai, H. Duan, H. Rong, D. Wang, L. Li, W. He, Y. Li, *ACS Catal.* **2013**, *3*, 608-612.
 [19] W. Zhang, F. Tan, W. Wang, X. Qiu, X. Qiao, J. Chen, *J. Hazard. Mater.* **2012**, *217*, 36-42.
 [20] S. Saha, A. Pal, S. Kundu, S. Basu, T. Pal, *Langmuir* **2009**, *26*, 2885-2893.
 [21] W. Dong, S. Cheng, C. Feng, N. Shang, S. Gao, C. Wang, *Catal. Commun.* **2017**, *90*, 70-74.
 [22] W. Ye, J. Yu, Y. Zhou, D. Gao, D. Wang, C. Wang, D. Xue, *Appl. Catal. B: Environ.* **2016**, *181*, 371-378.
 [23] X. Qiao, Z. Zhang, F. Tian, D. Hou, Z. Tian, D. Li, Q. Zhang, *Cryst. Growth Des.* **2017**, *17*, 3538-3547.
 [24] S. Patra, A. Naik, A. Pandey, D. Sen, S. Mazumder, A. Goswami, *Appl. Catal. A* **2016**, *524*, 214-222.
 [25] M. Hoffmann, S. Martin, W. Choi, D. Bahnemann, *Chem. Rev.* **1995**, *95*, 69-96.
 [26] A. Mills, S. Hunte, *J. photoch. photobio. A* **1997**, *108*, 1-35.
 [27] J. Schneider, M. Matsuoka, M. Takeuchi, J. Zhang, Y. Horiuchi, M. Anpo, D. Bahnemann, *Chem. Rev.* **2014**, *114*, 9919-9986.
 [28] S. Gazi, R. Ananthakrishnan, *Appl. Catal. B: Environ.* **2011**, *105*, 317-325.
 [29] A. Hernández-Gordillo, M. Arroyo, R. Zanella, V. Rodríguez-González, *J. Hazard. Mater.* **2014**, *268*, 84-91.
 [30] C. Castañeda, F. Tzompantzi, R. Gómez, *J. Sol-Gel Sci. Technol.* **2016**, *80*, 426-435.
 [31] T. Wu, P. Wang, J. Qian, Y. Ao, C. Wang, J. Hou, *Dalton Trans.* **2017**, *46*, 13793-13801.
 [32] Y. Nie, F. Yu, L. Wang, Q. Xing, X. Liu, Y. Pei, S. Suib, *Appl. Catal. B: Environ.* **2018**, *227*, 312-321.
 [33] J. Zou, L. Wang, J. Luo, Y. Nie, Q. Xing, X. Luo, S. Suib, *Appl. Catal. B: Environ.* **2016**, *193*, 103-109.
 [34] H. Shi, G. Chen, C. Zhang, Z. Zou, *ACS Catal.* **2014**, *4*, 3637-3643.
 [35] M. Marszewski, S. Cao, J. Yu, M. Jaroniec, *Mater. Horiz.* **2015**, *2*, 261-278.
 [36] J. Fu, Y. Tian, B. Chang, F. Xi, X. Dong, *J. Mater. Chem.* **2012**, *22*, 21159-21166.
 [37] Y. Tian, B. Chang, J. Lu, J. Fu, F. Xi, X. Dong, *ACS Appl. Mater. Interfaces* **2013**, *5*, 7079-7085.
 [38] X. Jiang, Q. Xing, X. Luo, F. Li, J. Zou, S. Liu, X. Wang, *Appl. Catal. B: Environ.* **2018**, *228*, 29-38.
 [39] G. Zhou, M. Wu, Q. Xing, F. Li, H. Liu, X. Luo, A. Zhang, *Appl. Catal. B: Environ.* **2018**, *220*, 607-614.

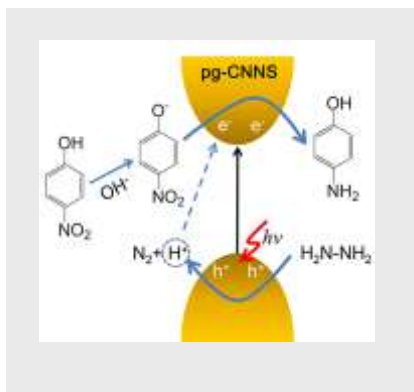
- [40] Y. Fu, T. Huang, B. Jia, J. Zhu, X. Wang, *Appl. Catal. B: Environ.* **2017**, *202*, 430-437.
- [41] W. Fang, Y. Deng, L. Tang, G. Zeng, Y. Zhou, X. Xie, J. Wang, *J. Colloid Interface Sci.* **2017**, *490*, 834-843.
- [42] P. Fageria, S. Uppala, R. Nazir, S. Gangopadhyay, C. Chang, M. Basu, S. Pande, *Langmuir* **2016**, *32*, 10054-10064.
- [43] Y. Wang, X. Wang, M. Antonietti, *Angew. Chem. Int. Edit.* **2012**, *51*, 68-89.
- [44] F. Cheng, H. Wang, X. Dong, *Chem. Commun.* **2015**, *51*, 7176-7179.
- [45] L. Zhang, D. Liu, J. Guan, X. Chen, X. Guo, F. Zhao, T. Hou, X. Mu, *Mater. Res. Bull.* **2014**, *59*, 84-92.
- [46] W. Ong, L. Tan, S. Chai, S. Yong, A. Mohamed, *Nano Energy* **2015**, *13*, 757-770.
- [47] P. Suyana, K. Sneha, B. Nair, V. Karunakaran, A. Mohamed, K. Warriar, U. Hareesh, *RSC Adv.* **2016**, *6*, 17800-17809.
- [48] X. Dai, M. Xie, S. Meng, X. Fu, S. Chen, *Appl. Catal. B: Environ.* **2014**, *158*, 382-390.
- [49] S. Ganesh Babu, R. Vinoth, P. Surya Narayana, D. Bahnemann, B. Neppolian, *APL Mater.* **2015**, *3*, 104415.
- [50] A. Hernández-Gordillo, A. Romero, F. Tzompantzi, R. Gómez, *Appl. Catal. B: Environ.* **2014**, *144*, 507-513.
- [51] Z. Jiang, X. Lv, D. Jiang, J. Xie, D. Mao, *J. Mater. Chem. A* **2013**, *1*, 14963-14972.
- [52] S. Ibrahim, S. Chakrabarty, S. Ghosh, T. Pal, *ChemistrySelect* **2017**, *2*, 537-545.
- [53] S. Mansingh, R. Acharya, S. Martha, K. Parida, *Phys. Chem. Chem. Phys.* **2018**, *20*, 9872-9885.
- [54] D. Guerrero-Araque, P. Acevedo-Peña, D. Ramírez-Ortega, R. Gómez, *New J. Chem.* **2017**, *41*, 12655-12663.
- [55] N. Tian, H. Huang, C. Liu, F. Dong, T. Zhang, X. Du, S. Yu, Y. Zhang, *J. Mater. Chem. A* **2015**, *3*, 17120-17129.
- [56] H. Zhao, H. Yu, X. Quan, S. Chen, Y. Zhang, H. Zhao, H. Wang, *Appl. Catal. B: Environ.* **2014**, *152*, 46-50.
- [57] J. Qian, C. Shen, J. Yan, F. Xi, X. Dong, J. Liu, *J. Phys. Chem. C* **2018**, *22*, 349-358.
- [58] Z. Yang, J. Li, F. Cheng, Z. Chen, X. Dong, *J. Alloy. Compd.* **2015**, *634*, 215-222.

Entry for the Table of Contents (Please choose one layout)

Layout 1:

FULL PAPER

The pg-CNNS photocatalyst prepared by sulphuric acid exfoliation of g-C₃N₄ possesses 2D ultrathin morphology that is favorable for efficient separation of photo-excited charges and then fast diffusion to surface of catalyst. Furthermore, plentiful positive charges on surface promote adsorption of *p*-nitrophenolate anions and subsequently rapid reduction of PNP to PAP by photo-generated electrons. Additionally, the pg-CNNS has well photocatalytic reusability and superb activity for reduction of other functionalized nitroaromatic chemicals.



Jiajia Qian, Aili Yuan, Chengkai Yao,
Jiyang Liu, Benxia Li, Fengna Xi,
Xiaoping Dong*

Page No. – Page No.

Highly efficient photo-reduction of *p*-nitrophenol by protonated graphitic carbon nitride nanosheets